Poly(ethylene terephthalate) Nanocomposite Fibers by *In Situ* Polymerization: The Thermomechanical Properties and Morphology

Jin-Hae Chang,[1] Mu Kyung Mun,[1] Ihn Chong Lee[2]

[1]*Department of Polymer Science and Engineering, Gumoh National Institute of Technology, Kumi 730-701, South Korea*
[2]*Department of Chemistry, Hallym University, Chunchon 200-702, South Korea*

Received 11 November 2004; accepted 2 March 2005
DOI 10.1002/app.22382
Published online in Wiley InterScience (www.interscience.wiley.com).

ABSTRACT: A series of nanocomposites of poly(ethylene terephthalate) (PET) with the organoclay dodecyltriphenylphosphonium-mica (C_{12}PPh-mica) were synthesized with the *in situ* polymerization method. PET hybrid fibers with various organoclay concentrations were melt-spun at various draw ratios (DRs) to produce monofilaments. The thermomechanical properties and morphologies of the PET hybrid fibers were characterized with differential scanning calorimetry, thermogravimetric analysis, wide-angle X-ray diffraction, electron microscopy, and universal tensile analysis. The organoclay was intercalated in the polymer matrix at all magnification levels, and some of the agglomerated organoclay layers were greater than 50 nm thick. The thermal stabilities and initial tensile moduli of the hybrid fibers increased with an increasing clay content for DR = 1. For DR = 1, the ultimate tensile strengths of the PET hybrid fibers increased with the addition of clay up to a critical clay loading and then decreased above that critical concentration. However, the tensile mechanical properties of the hybrid fibers did not improve with increasing DR. © 2005 Wiley Periodicals, Inc. J Appl Polym Sci 98: 2009–2016, 2005

Key words: fibers; nanocomposites; organoclay; polyesters

INTRODUCTION

Organic/inorganic hybrids have generated substantial recent interest as a result of their potential as single molecular-scale composites with desirable organic and inorganic characteristics and new properties arising from the interaction between the two components.[1–4] By the addition of a few weight percent of an inorganic clay to a polymer matrix, the resulting nanoscale composites have been found to exhibit significant improvements in many properties in comparison with those of the polymer matrix, such as their mechanical and thermal properties, and in their flame retardance.[5–9] Furthermore, the incorporation of clay can result in materials possessing excellent gas-barrier properties with far less inorganic content than conventionally filled polymer composites have.[10,11]

Of the various methods used in the preparation of polymer/clay nanocomposites, *in situ* intercalation polymerization enables significant control over both the polymer architecture and the final structure of the composite. The *in situ* intercalation polymerization technique is also particularly attractive because of its versatility and compatibility with the use of reactive monomers, and it is beginning to be used in commercial applications.[12–15]

Poly(ethylene terephthalate) (PET) is a semicrystalline polymer possessing excellent chemical resistance, thermal stability, melt mobility, and spinnability.[16,17] It is used in such diverse fields as the packaging, electrical, automotive, and construction industries. The melt polymerization process for producing PET has two steps. The first step is the transesterification of dimethyl terephthalate (DMT) with 1,2-ethylene glycol (EG) or the esterification of terephthalic acid with EG. The second step is the polycondensation of the transesterification or esterification product *in vacuo*, which removes the polycondensation byproducts, namely, EG and methanol, until the desired molecular weight is reached.

The objective of this study was to evaluate the variation of the properties of PET nanocomposites as a function of their organoclay content. Alkylammonium derivatives of mica-type layered organoclays have been employed in a wide variety of industrial and scientific applications. However, we have found in previous research that severe degradation of these materials occurs during processing because of the high processing temperature of PET.[18–21] In this study, we used a thermally stable phosphonium derivative of

Correspondence to: J.-H. Chang (changjinhae@hanmail.net).
Contract grant sponsor: Hallym University Research Fund (2003).

TABLE I
Thermal Properties of the PET Hybrid Fibers

Organoclay (wt %)	DR	IV[a]	T_g (°C)	T_m (°C)	T_D^i (°C)	wt_R^{600b} (%)
(pure PET)	1	1.02	71	245	370	1
1	1	0.86	71	246	383	17
2	1	0.98	75	245	385	18
3	1	0.97	75	246	387	19
5	1	0.94	67	227	389	22
5	3		67	226	389	22
5	10		67	228	389	22
5	16		67	227	389	22

[a] Inherent viscosity measured at 30°C with 0.1 g/100 mL solutions in a phenol/1,1,2,2-tetrachloroethane (50/50 = w/w) mixture.
[b] Weight percentage of residue at 600°C.

organomica to obtain PET hybrid fibers without the occurrence of thermal degradation during processing. In this article, we describe a new method for making PET nanocomposites with *in situ* intercalation polymerization. Furthermore, we report the variations of the thermomechanical properties and morphologies of the PET nanocomposite fibers with the organoclay content and draw ratio (DR).

EXPERIMENTAL

Materials

Na^+-type fluorinated synthetic mica (Na^+-mica), in which the free OH groups of mica are replaced by fluorine, was supplied by CO-OP, Ltd. (Tokyo, Japan). Its cation-exchange capacity was 70–80 mequiv/100 g. All reagents were purchased from TCI, Junsei Chemical Co. (Tokyo, Japan), and Aldrich Chemical Co. (Seoul, Korea) The commercially available solvents were purified with distillation.

Preparation of the organoclay

The organically modified mica, C_{12}PPh-mica, used in this study was synthesized with an ion-exchange reaction between Na^+-mica and dodecyltriphenylphosphonium chloride (C_{12}PPh-Cl^-).[15] The chemical structure of C_{12}PPh-mica is as follows:

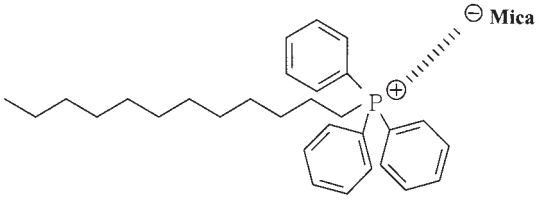

Preparation of the C_{12}PPh-mica/PET nanocomposites

All the samples were prepared as melts. Because the synthetic procedures for the hybrids were very similar, only a representative example, the procedure for the preparation of the nanocomposite containing 2 wt % organoclay, is described here. EG (62 g, 1.0 mol) and 1.96 g of C_{12}PPh-mica were placed in a polymerization tube, and the mixture was stirred for 30 min at room temperature. DMT (97 g, 0.5 mol) and a few drops (1.2×10^{-4} mol) of isopropyl titanate were placed in a separate tube, and this mixture was added to the organoclay–EG system with vigorous stirring to obtain a homogeneously dispersed system. This mixture was heated at first for 1 h at 190°C under a steady stream of N_2 gas. The reaction mixture was then heated to 230°C and maintained at that temperature for 2 h under a steady stream of N_2 gas. During this period, the continuous generation of methanol was observed. Finally, the mixture was heated for 2 h at 280°C at a pressure of 1 Torr. The product was cooled to room temperature, repeatedly washed with water, and dried *in vacuo* at 70°C for 1 day to obtain the PET hybrid. The polymers were soluble in mixed solvents, so a mixed solvent of phenol and 1,1,2,2-tetrachloroethane (50/50 w/w) was used in the measurement of the solution viscosity. The inherent solution viscosities (see Table I) ranged from 0.86 to 1.02.

Extrusion

The composites were pressed at 270°C and 2500 kg/cm^2 for 2–3 min on a hot press. The ~0.5-mm-thick films obtained were dried in a vacuum oven at 80°C for 24 h and then extruded through the die of a capillary rheometer. The hot extrudates were stretched through the die of the capillary rheometer (model 5460, Instron, High Wycombe, England) at 270°C and immediately drawn at the constant speed of the take-up machine to form fibers. The pure PET and PET hybrids were extruded with various DRs, and the thermal and tensile mechanical properties of the extrudates were examined. The standard die diameter (DR = 1) was 0.75 mm. When the organoclay content of the hybrids was increased from 0 to 5 wt %, all

fibers obtained from the capillary rheometer were bright yellow. The DR was calculated from the ratio of the velocity of extrusion to the take-up speed. The mean residence time in the capillary rheometer was ~3–4 min.

Characterization

The thermal behavior of these materials was investigated with a DuPont model 910 differential scanning calorimeter (Wilmington, DE) and a thermogravimetric analyzer at a heating rate of 20°C/min under a flow of N_2. Wide-angle X-ray diffraction (WAXD) measurements were performed at room temperature with a Rigaku D/Max-IIIB X-ray diffractometer (Tokyo, Japan) with Ni-filtered Co Kα radiation. The scanning rate was 2°/min over a 2θ range of 2–15°.

The tensile properties of the fibers were determined with an Instron model 5564 mechanical tester at a crosshead speed of 20 mm/min at room temperature. The experimental uncertainties in the tensile strength and the modulus were ±1 MPa and ±0.05 GPa, respectively. The reported properties were obtained as the average of at least 10 individual determinations.

The morphologies of the fractured surfaces of the extruded fibers were investigated with a Hitachi S-2400 scanning electron microscope (Tokyo, Japan). An SPI sputter coater (Tokyo, Japan) was used to sputter-coat the fractured surfaces with gold for enhanced conductivity. The samples were prepared by the placement of the PET hybrid fibers into epoxy capsules and then the curing of the epoxy at 70°C for 24 h *in vacuo*. The cured epoxies containing the PET hybrids were then microtomed into 90-nm-thick slices, and a layer of carbon, about 3 nm thick, was deposited on each slice on a 200-mesh copper net. Transmission electron microscopy (TEM) photographs of ultrathin sections of the polymer/organoclay hybrid samples were obtained with an EM 912 Omega transmission electron microscope (Oberkochen, Germany) with an acceleration voltage of 120 kV.

RESULTS AND DISCUSSION

WAXD

X-ray diffraction (XRD) is very useful for measuring the *d*-spacing of ordered immiscible and ordered intercalated polymer nanocomposites. The basal spacings of the pristine clay and the organoclay are shown in Figure 1. Each curve has one peak, corresponding to basal spacings of 9.57 (2θ = 10.76°) and 27.63 Å (2θ = 3.68°) for Na^+-mica and C_{12}PPh-mica, respectively. As expected, the ion exchange between the clay (Na^+-mica) and C_{12}PPh-Cl^- resulted in an increase in the basal interlayer spacing over that of pristine Na^+-mica and in a large shift of the diffraction peak toward lower values of 2θ.[22–24] When the clay was modified with this organic compound, it exhibited improved compatibility with the polymer, so the clay galleries could easily be intercalated with the polymer. In general, larger gallery spacings normally translate into increased dispersion and delamination in polymers.

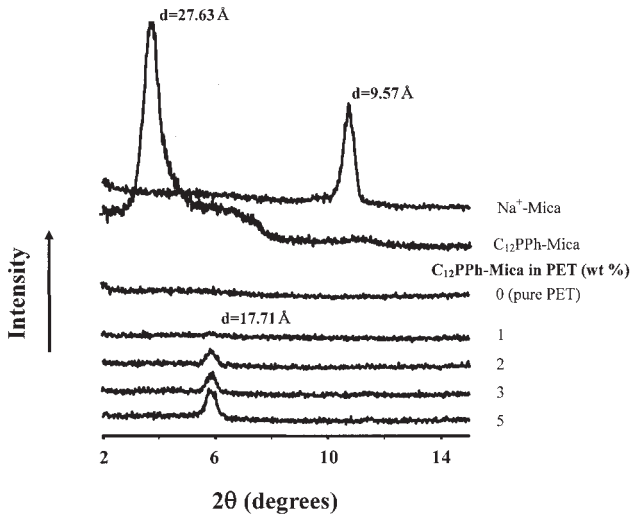

Figure 1 XRD patterns for clay, organoclay, and PET hybrid fibers with various organoclay contents.

The XRD results for the PET nanocomposite fibers with organoclay concentrations varying in the range of 0–5 wt % are shown in Figure 1. For PET with 1 wt % organoclay, there is only a weak peak at d = 17.71 Å (2θ = 5.74°). A substantial increase in the intensity of this XRD peak can be observed for clay loadings in the range of 1–5 wt %, and this suggests that the dispersion is better at lower clay loadings than at higher clay loadings and that agglomeration occurs at higher clay loadings. However, the presence of the organoclay had no effect on the location of the peak, and this indicates that perfect exfoliation of the clay layer structure of the organoclay in PET did not occur in these nanocomposites.[25]

Figure 2 shows the XRD curves for PET nanocomposites containing 5 wt % organoclay with various DRs. A peak at d = 17.71 Å (2θ = 5.74°) was found in the XRD results for the extrudate fibers with DR = 1. When DR was increased from 1 to 16, the intensity of this peak decreased gradually. It has previously been suggested that increasing the stretching of the fiber during extrusion results in a disordered crystalline structure of clay in a polymer matrix.[15]

Morphology

Because of the differences in the scattering densities of the clay and the PET matrix polymer, the clay agglomerates could easily be imaged with scanning electron microscopy (SEM). SEM images of the fractured sur-

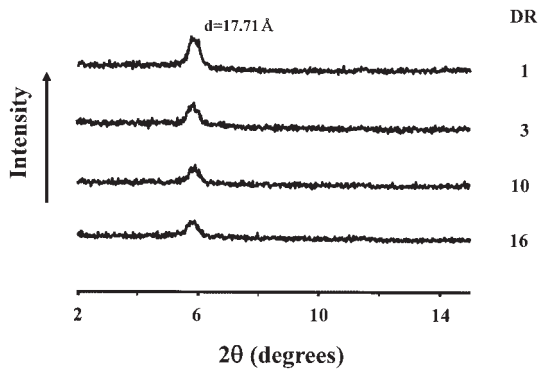

Figure 2 XRD patterns for PET hybrid fibers with different DRs and 5 wt % C_{12}PPh-mica.

faces of the PET hybrid fibers containing 0–5 wt % organoclay are compared in Figures 3 and 4. Figure 3 shows that clay phases form in the undrawn hybrid fibers: the fibers with 0–5 wt % C_{12}PPh-mica have morphologies consisting of clay domains, 70–100 nm in size, that are well dispersed in a continuous PET phase. The particles of the dispersed clay phase were easily detected for clay concentrations in the range of 1–5 wt %. Figure 4 shows micrographs taken of 5 wt % C_{12}PPh-mica/PET hybrid fibers with DRs ranging from 1 to 16. The 5 wt % hybrid fiber with DR = 3 contains fine clay phases 60–80 nm in diameter [see Fig. 4(b)]. The hybrid fiber with DR = 16 also exhibits fine dispersion with domains 40–70 nm in diameter [see Fig. 4(d)]. The domain size of the dispersed clay phase decreases with increasing DR. This decline in the domain size seems to be the result of excess stretching of the fibers when the extrudates pass through the capillary rheometer.[26–29]

More direct evidence of the formation of true nanocomposites is provided by the TEM images of an ultramicrotomed section. Figure 5(a–c) shows photographs of PET hybrid fibers containing 5 wt % organoclay with DR = 1; the magnification level increases from micrograph a to micrograph c. The dark lines are the intersections of 1-nm-thick sheet layers. Figure 5 shows that the organoclay is intercalated (not exfoliated) in the polymer matrix at all magnification levels and that some of the agglomerated organoclay layers are greater than 50 nm thick. The peaks in the XRD patterns of these samples should be attributed to these agglomerated layers (see Figs. 1 and 2).

Thermal behaviors

The thermal behaviors of pure PET and the hybrid fibers obtained with various DRs are listed in Table I. The glass-transition temperature (T_g) of the PET hybrid fibers increased linearly from 71 to 75°C with increases in the clay loading from 0 to 3 wt %. The increase in T_g of these hybrids could be due to two different factors. First, the effect of small amounts of dispersed clay layers on the free volume of PET is

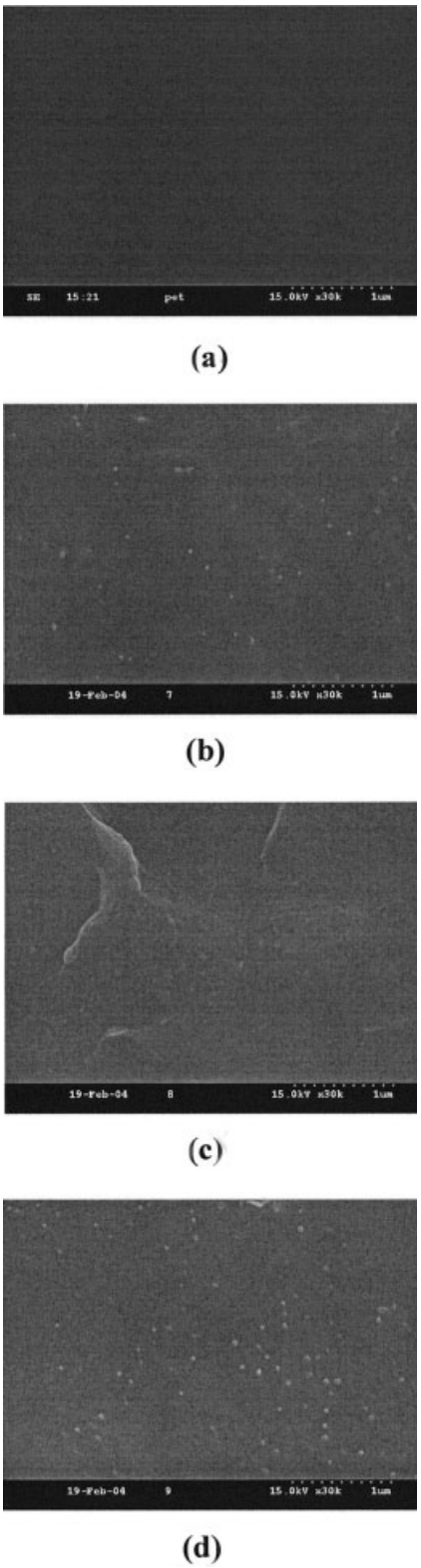

Figure 3 SEM micrographs of PET hybrid fibers containing (a) 0 (pure PET), (b) 1, (c) 2, and (d) 5 wt % C_{12}PPh-mica.

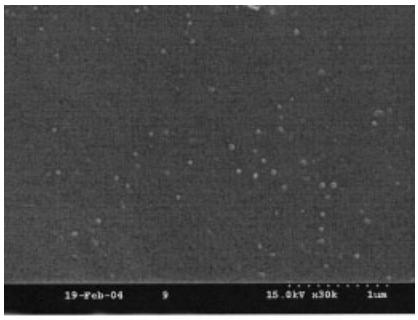

(a)

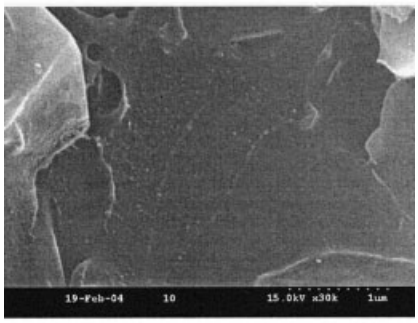

(b)

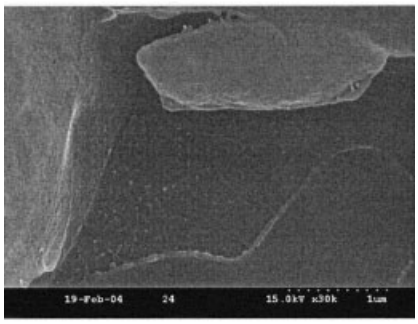

(c)

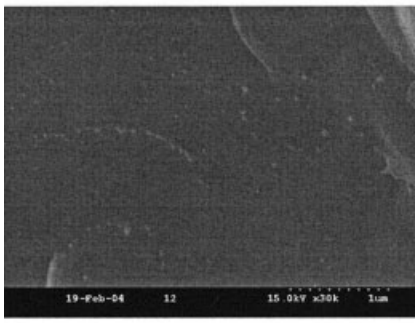

(d)

Figure 4 SEM micrographs of PET hybrid fibers with 5 wt % C_{12}PPh-mica and DRs of (a) 1, (b) 3, (c) 10, and (d) 16.

significant and influences T_g of the PET hybrids. The second factor is the confinement within the clay galleries of the intercalated polymer chains, which prevents their segmental motions. T_g of the PET hybrid fibers decreased from 75 to 67°C when the organoclay loading in the PET matrix was increased from 3 to 5 wt

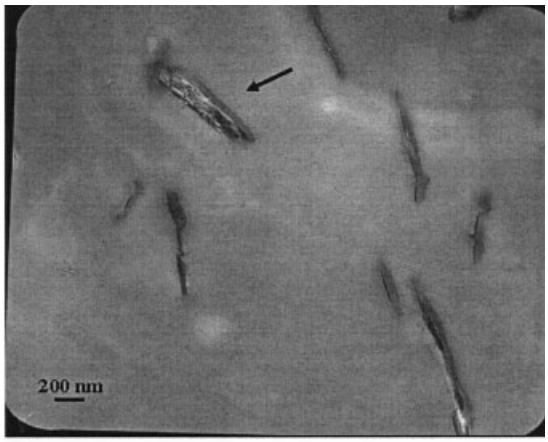

(a)

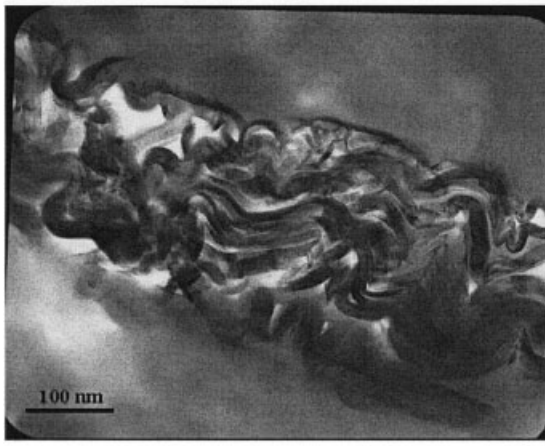

(b)

(c)

Figure 5 TEM micrographs of PET hybrid fibers with 5 wt % C_{12}PPh-mica and DR = 1, with the magnification level increasing from micrograph a to c.

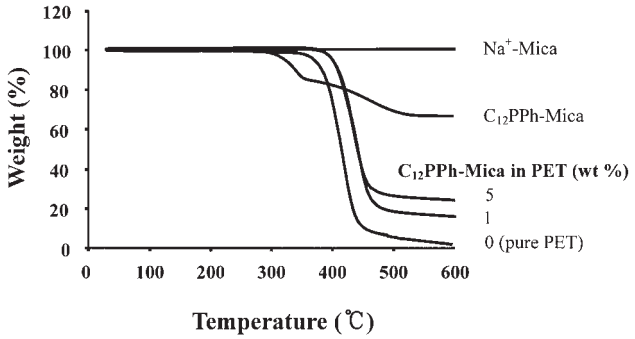

Figure 6 TGA thermograms of clay, organoclay, and PET hybrid fibers with different organoclay content.

%. This decrease in T_g seems to be the result of clay agglomeration, which occurs for the addition of clay to the polymer matrix above a critical clay loading.[30–32]

The endothermic peak for pure PET appears at 245°C and corresponds to its melting-transition temperature (T_m). The T_m values of the hybrid fibers were fairly constant in the range of 245–246°C when the clay loading was increased from 0 to 3 wt % and then decreased to 227°C with 5 wt % clay. This suggests that the 5 wt % organoclay domains may be more poorly dispersed in the PET matrix than the 3 wt % organoclay domains. In other words, a higher organoclay content leads to the agglomeration of clay particles, which reduces the heat insulation effect of the clay layers in the polymer matrix.[14,33] This evidence for organoclay agglomeration in PET was confirmed with XRD and TEM (see Figs. 1 and 5).

The initial thermal degradation temperature (T_D^i) of the C_{12}PPh-mica/PET hybrid fibers increased with their organoclay concentration. The thermogravimetric analysis (TGA) results for pure PET and PET hybrid fibers with 0–5 wt % C_{12}PPh-MMT are shown in Table I and Figure 6. Table I shows that T_D^i (2% weight loss) for PET hybrid fibers with clay compositions of 0–5 wt % are in the range of 370–389°C; the highest value was obtained for 5 wt % C_{12}PPh-mica/PET. The increases in T_D^i of these hybrid fibers with the organoclay content could be due to many different factors, particularly the high thermal stability of the clay and the interaction between the clay particles and the polymer matrix. Similar trends have been noted in other articles.[34–36] A further factor could be the mass-transport barrier introduced by the clay particles to the volatile products generated during decomposition.[37,38]

The weight of the residue at 600°C increased from 1 to 22% with increases in the clay loading from 0 to 5%. This enhancement of char formation was ascribed to the high heat resistance of the clay.

For the PET hybrid fibers containing 5 wt % organoclay, the overall thermal properties were unchanged with increases in DR from 1 to 16. We conclude that the thermal properties of the PET hybrid fibers were not affected by increases in the stretching of the fiber during spinning.

Mechanical properties

Pure PET and the PET hybrids were extruded through a capillary die at various DRs to examine the tensile strengths and moduli of the extrudates with DR. The tensile mechanical properties of PET and the hybrid fibers are given in Table II. At DR = 1, the ultimate tensile strength of the C_{12}PPh-mica hybrid fibers increased with the addition of clay up to a critical content and then decreased above that critical loading. For example, the strength of 1 wt % PET hybrid fibers was 72 MPa, which was about 60% higher than that of pure PET (46 MPa). When the PET organoclay content reached 5 wt %, the strength decreased to 55 MPa. This decrease in the ultimate tensile strength was mainly due to the agglomeration of clay particles above a critical organoclay content, as we have described in another article.[39,40] Evidence for clay agglomeration was also obtained with XRD, SEM, and TEM, as shown in Figures 1, 3, and 5, respectively.

However, the initial modulus monotonically increased with an increasing PET matrix organoclay content (see Table II). At DR = 1, the initial modulus increased from 2.21 to 3.40 GPa with linear increases in the C_{12}PPh-mica content up to 5 wt %. This enhancement of the modulus was ascribed to the high

TABLE II
Tensile Properties of the PET Hybrid Fibers

Organoclay (wt %)	DR	Ultimate strength (MPa)	Initial modulus (GPa)	EB (%)
0 (pure PET)	1	46	2.21	3
	3	47	2.24	3
	10	51	2.28	3
	16	51	2.39	2
1	1	72	2.90	2
	3	72	2.88	3
	10	71	2.83	3
	16	71	2.85	3
2	1	64	3.10	2
	3	62	3.11	3
	10	63	3.13	3
	16	64	3.09	3
3	1	60	3.18	2
	3	57	3.22	3
	10	58	3.20	3
	16	62	3.23	3
5	1	55	3.40	3
	3	56	3.39	2
	10	56	3.37	2
	16	57	3.38	2

EB = elongation at break.

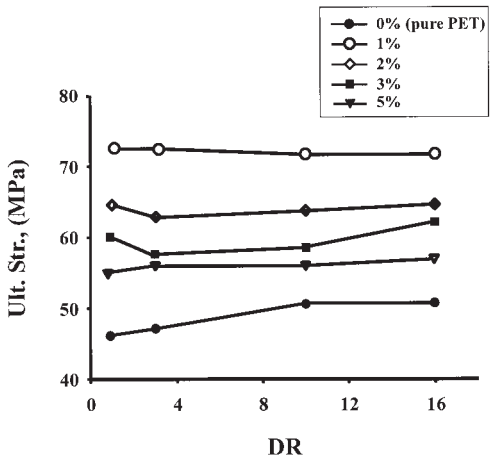

Figure 7 Effects of DR on the ultimate tensile strength of the organoclay content.

resistance exerted by the clay. Furthermore, the increased stretching resistance of the polymer chains produced by the orientation of their backbones in the galleries also contributed to the enhancement of the modulus. This trend is consistent with results reported elsewhere.[41,42] According to Kojima et al.,[42] regions in a polymer/clay hybrid in which the polymer chains are restricted in mobility make significant contributions to a hybrid's tensile modulus. Thus, increasing the clay content increases the restriction of the polymer chains' mobility and results in an increase in the tensile modulus.

The elongation percentages required for breaking the hybrid fibers were all in the range of 2–3%. These values were constant for organoclay loadings in the range of 1–5 wt %.

On the basis of the aforementioned results, we conclude that these enhancements of the mechanical properties can be directly attributed to the reinforcement provided by the intercalation of PET in clay galleries and by the dispersion of clay particles in the polymer matrix. The improvements in the tensile properties produced by the clay layers depend on the interactions between the rigid, rod-shaped polyester molecules and the layered clay, as well as the rigidity of the clay layers.

The variations in the tensile strengths and initial moduli with DR were insignificant for pure PET, as is usually the case for flexible, coil-like polymers. For pure PET, as shown in Table II, the strength and the modulus increased from 46 to 51 MPa and from 2.21 to 2.39 GPa, respectively, as DR was increased from 1 to 16.

The tensile mechanical properties of the PET hybrid fibers did not improve with increasing DR. Similar trends were observed for all of the hybrids containing 1–5 wt % organoclay for increases in DR from 1 to 16. The variations in the ultimate strengths and initial moduli of the hybrids with DR are plotted in Figures 7 and 8, respectively. An increase in the mechanical tensile strength with increasing DR is very common for engineering plastics and is usually observed for flexible, coil-like polymers.[43,44] However, our system did not follow this trend. This tensile property seems to be the result of poor interfacial interaction between the organoclay and the matrix polymer, and this means that increasing the stretching of the PET hybrid fibers during spinning is not effective in producing a better extension of the polymer matrix. Many researchers[45–47] have reported that an imperfect incursion/matrix interface cannot sustain the large interfacial shear stress that develops as a result of an applied strain. The elongation at break of the hybrids was virtually unchanged, remaining in the range of 2–3% as DR was increased from 1 to 16.

CONCLUSIONS

PET/C_{12}PPh-mica hybrids were prepared with the *in situ* intercalation polymerization method. Hybrids with various organoclay content were extruded with various DRs from a capillary rheometer to investigate the variation of their thermomechanical properties and morphologies with DR. We used SEM and TEM to confirm that the organoclays were intercalated, and some of them were agglomerated within the polymer matrix at all magnification levels. T_g of the hybrid fibers increased with the addition of organoclay up to a critical organoclay content (3 wt %) and then decreased with further increases in the organoclay content. However, T_D^i monotonically increased for all increases in the PET matrix organoclay content that we studied. These thermal properties were unchanged with variations in DR from 1 to 16 for the PET hybrid fibers containing 5 wt % C_{12}PPh-mica.

The ultimate tensile strength of the hybrid fibers increased with increases in the C_{12}PPh-mica content

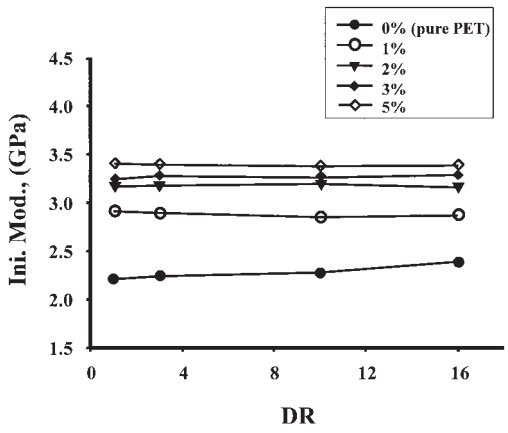

Figure 8 Effects of DR on the initial tensile modulus of the organoclay content.

up to 1 wt % and then decreased with further organoclay loading. However, the initial modulus gradually increased with increasing organoclay content at DR = 1. The tensile properties of the hybrid fibers were better than those of the matrix polymer for all compositions that we tested. However, the tensile mechanical properties of the PET hybrid fibers did not improve with increases in DR.

Overall, the addition of small amounts of C_{12}PPh-mica to PET to create PET hybrid fibers improved the thermomechanical properties of the fibers. We conclude that the properties of the clay particles affected the thermal behavior and tensile mechanical properties of the polymer/clay hybrid fibers.

References

1. Giannelis, E. P. Adv Mater 1996, 8, 29.
2. Messersmith, P. B.; Giannelis, E. P. Chem Mater 1993, 5, 1064.
3. Pinnavaia, T. J. Science 1983, 220, 365.
4. Gilman, J. W. Appl Clay Sci 1999, 15, 31.
5. Wang, Z.; Lan, T.; Pinnavaia, T. J. Chem Mater 1996, 8, 2200.
6. Chang, J.-H.; An, Y. U.; Sur, G. S. J Polym Sci Part B: Polym Phys 2003, 41, 94.
7. Akelah, A.; Moet, A. J Mater Sci 1996, 31, 3589.
8. Okada, A.; Usuki, A. Mater Sci Eng C 1995, 3, 109.
9. Kojima, Y.; Usuki, A.; Kawasumi, M.; Okada, A.; Kurauchi, T.; Kamigaito, O. J Polym Sci Part A: Polym Chem 1993, 31, 1755.
10. Osman, M. A.; Mittal, V.; Morbidelli, M.; Suter, U. W. Macromolecules 2003, 36, 9851.
11. Bharadwaj, R. K. Macromolecules 2001, 34, 9189.
12. Hwang, S. H.; Paeng, S. W.; Kim, J. Y.; Huh, W. Polym Bull 2003, 49, 329.
13. Wang, D.; Zhu, J.; Yao, Q.; Wilkie, C. A. Chem Mater 2002, 14, 3837.
14. LeBaron, P. C.; Wang, Z.; Pinnavaia, T. J. Appl Clay Sci 1999, 12, 11.
15. Chang, J.-H.; Kim, S. J.; Im, S. Polymer 2004, 45, 5171.
16. Bang, H. J.; Lee, J. K.; Lee, K. H. J Polym Sci Part B: Polym Phys 2000, 38, 2625.
17. Wasiak, A.; Sajkiewicz, P.; Wozniak, A. J Polym Sci Part B: Polym Phys 1999, 37, 2821.
18. Zhu, J.; Morgan, A. B.; Lamelas, F. J.; Wilkie, C. A. Chem Mater 2001, 13, 3774.
19. Zhu, J.; Uhl, F. M.; Morgan, A. B.; Wilkie, C. A. Chem Mater 2001, 13, 4649.
20. Saujanya, C.; Imai, Y.; Tateyama, H. Polym Bull 2002, 49, 69.
21. Davis, C. H.; Mathias, L. J.; Gilman, J. W.; Schiraldi, D. A.; Shields, J. R.; Trulove, P.; Sutto, T. E.; Delong, H. C. J Polym Sci Part B: Polym Phys 2002, 40, 2661.
22. Chang, J.-H.; An, Y. U. J Polym Sci Part B: Polym Phys 2002, 40, 670.
23. Hsiao, S. H.; Liou, G. S.; Chang, L. M. J Appl Polym Sci 2001, 80, 2067.
24. Ke, Y.; Lu, J.; Yi, X.; Zhao, J.; Qi, Z. J Appl Polym Sci 2000, 78, 808.
25. Morgan, A. B.; Gilman, J. W. J Appl Polym Sci 2003, 87, 1329.
26. Kohli, A.; Chung, N.; Weiss, R. A. Polym Eng Sci 1989, 29, 573.
27. Dutta, D.; Fruitwala, H.; Kohli, A.; Weiss, R. A. Polym Eng Sci 1990, 30, 1005.
28. Blizard, K. G.; Baird, D. G. Polym Eng Sci 1987, 27, 653.
29. Weiss, R. A.; Huh, W.; Nicolais, L. Polym Eng Sci 1987, 27, 684.
30. Xu, H.; Kuo, S.-W.; Lee, J.-S.; Chang, F.-C. Macromolecules 2002, 35, 8788.
31. Haddad, T. S.; Lichtenhan, J. D. Macromolecules 1996, 29, 7302.
32. Agag, A.; Takeichi, T. Polymer 2000, 41, 7083.
33. Hussain, M.; Varley, R. J.; Mathys, Z.; Cheng, Y. B.; Simon, G. P. J Appl Polym Sci 2004, 91, 1233.
34. Fischer, H. R.; Gielgens, L. H.; Koster, T. P. M. Acta Polym 1999, 50, 122.
35. Petrovic, X. S.; Javni, L.; Waddong, A.; Banhegyi, G. J. J Appl Polym Sci 2000, 76, 33.
36. Zhu, Z. K.; Yang, Y.; Yin, J.; Wang, X.; Ke, Y.; Qi, Z. J Appl Polym Sci 1999, 3, 2063.
37. Chang, J.-H.; Seo, B. S.; Hwang, D. H. Polymer 2002, 43, 2969.
38. Fornes, T. D.; Yoon, P. J.; Hunter, D. L.; Keskkula, H.; Paul, D. R. Polymer 2002, 43, 5915.
39. Chang, J.-H.; Park, D.-K.; Ihn, K. J. J Polym Sci Part B: Polym Phys 2001, 39, 471.
40. Chang, J.-H.; Park, K. D.; Cho, D.; Yang, H. S.; Ihn, K. J. Polym Eng Sci 2001, 41, 1514.
41. Chen, L.; Wong, S.-C.; Pisharath, S. J Appl Polym Sci 2003, 88, 3298.
42. Kojima, Y.; Usuki, A.; Kawasumi, M.; Okada, A.; Fukushima, Y.; Kurauchi, T.; Kamigaito, O. J Mater Res 1993, 8, 1185.
43. La Mantia, F. P.; Valenza, A.; Paci, M.; Magagnini, P. L. J Appl Polym Sci 1989, 38, 583.
44. Chang, J.-H.; Jo, B. Y. J Appl Polym Sci 1996, 60, 939.
45. Chawla, K. K. Composite Materials Science and Engineering; Springer-Verlag: New York, 1987.
46. Curtin, W. A. J Am Ceram Soc 1991, 74, 2837.
47. Shia, D.; Hui, Y.; Burnside, S. D.; Giannelis, E. P. Polym Eng Sci 1987, 27, 887.